RSC Advances

PAPER

View Article Online
View Journal | View Issue

Cite this: *RSC Adv.*, 2025, **15**, 12954

Understanding the roles of stabilizers and reductants in soluble Pt nanoparticle catalysts for highly efficient hydrogenation of benzoic acid under mild conditions†

Hangyu Liu,[a] Xilei Tian,[a] Benlei Wang,[a] Chen Li,*[a] Guohong Tao,[b] Jing Du,[c] Ling He *[b] and Shaopeng Li *[c]

Received 8th March 2025
Accepted 9th April 2025

DOI: 10.1039/d5ra01663k

rsc.li/rsc-advances

Stabilizers and reductants of soluble metal nanoparticle (SMNP) catalysts have particular properties that differ from those of heterogeneous catalysts and can dramatically influence the activity of catalysts. To achieve better performances of SMNP catalysts, the functions of stabilizers and reductants have to be understood. Herein, we prepared a batch of SMNP catalysts by adjusting the amount of stabilizers and the type of reductants and found that the stabilizers and reductants will affect not only the size of catalysts but also the electronic states and accessibility of active metal sites, which determine the activity of catalysts. The SMNP catalyst prepared with a suitable stabilizer and reductant presents significantly higher catalytic activity with complete conversion in the selective hydrogenation of benzoic acid to cyclohexane carboxylic acid under mild conditions (30 °C and 1 atm H_2) than that of the conventional heterogeneous catalyst (Pt/C). Besides, one-step selective hydrogenation of various benzoic acid derivatives was carried out over the SMNP catalyst. These conclusions on the functions of stabilizers and reductants provide new insight into the preparation of high-efficiency SMNP catalysts.

Catalysis has greatly promoted the progress of human life and industrial production, where catalysts play a key role. Soluble metal nanoparticle (SMNP) catalysts have attracted increasing focus over the last decade.[1] Metal nanoparticle (MNP) catalysts stabilized by polymers, surfactants, or ionic liquids are soluble in green solvents (such as water and ionic liquids) and exhibit superior catalytic activities and selectivities for various reactions under mild conditions compared with traditional heterogeneous catalysts.[2] The distinct catalytic activity is mostly due to their high surface-to-volume ratio, corresponding high surface special active atom number, and less liquid–solid mass transfer and diffusion resistances in solutions. Besides, their controllable sizes and morphologies play important roles in catalytic reactions, usually influenced by the stabilizers and reductants added in the synthesis.[3] Stabilizers serve as structure-directing agents by interacting with MNPs and provide electrostatic and steric stabilizations for as-prepared MNPs.[4] Several reductants, including sodium borohydride ($NaBH_4$), ethanol, formaldehyde, hydrazine hydrate, play major roles in the formation of MNPs from metal salts.[5] In addition to the size, the electronic state and accessibility of active metal sites influenced by stabilizers and reductants can also affect the activity of the catalysts. Thus, the roles of stabilizers and reductants in SMNP catalysts need to be studied systematically.

To understand the effect of stabilizers and reductants on SMNP catalysts, we chose the selective hydrogenation of benzoic acid (BA) to cyclohexanecarboxylic acid (CCA) as the probe reaction, which has great industrial potential. Cyclohexanecarboxylic acid (CCA) is an important and versatile intermediate in the chemical and industrial processes, which has been used in the synthesis of pharmaceuticals, such as praziquantel, hexanolactam, and ansatrienin.[6] Moreover, CCA reacts with nitrosyl-sulfuric acid to produce caprolactam (the precursor of nylon), which is the basic reaction in the toluene-based caprolactam synthesis.[7] It is well known that the chemo-selective catalytic hydrogenation of BA is an efficient process to produce CCA, and many transition metals have been used as catalysts.[8] However, the high resonance energy of aromatic compounds and harsh reaction conditions (high H_2 pressure (10–100 atm) and high temperature (50–200 °C)) have become a troublesome problem in the hydrogenation of BA (Table S3†).[8] To meet the demands of industrial application and green chemistry, searching for more efficient catalysts for the

[a]*CenerTech Tianjin Chemical Research & Design Institute Company, Ltd, Tianjin 300131, P. R. China. E-mail: lichen6@cnooc.com.cn*

[b]*College of Chemistry, Sichuan University, Chengdu, 610064, P. R. China. E-mail: lhe@scu.edu.cn*

[c]*Department of Chemistry, Institute of Molecular Aggregation Science, Tianjin Key Laboratory of Molecular Optoelectronic Sciences, Tianjin University, Tianjin 300072, P. R. China. E-mail: lishaopeng@iccas.ac.cn*

† Electronic supplementary information (ESI) available. See DOI: https://doi.org/10.1039/d5ra01663k

hydrogenation of BA under mild conditions (room temperature and atmospheric pressure) is an important challenge for chemists.

Herein, a series of soluble Pt nanoparticle (SPtNP) catalysts were prepared by changing the added amount of stabilizers and the type of reductants in synthesis to study the functions of stabilizers and reductants. We found that the stabilizers and reductants will affect not only the size of catalysts but also the electronic state and accessibility of active metal sites. The SPtNP catalyst prepared with a suitable stabilizer and reductant presents significantly high catalytic activity for the one-step selective hydrogenation of BA to CCA in water without other co-catalysts under mild conditions (30 °C, 1 atm H_2, 3 h) (Scheme 1). The conclusions verified by this work can be extended to the preparation of other SMNP catalysts, providing new insight into the preparation of high-efficiency SMNP catalysts.

To prepare high-efficiency SPtNP catalysts, dihydrogen hexachloroplatinate (IV) hexahydrate (0.1 mmol) was first dispersed in 10 ml of water, to which a water solution (10 ml) containing polyvinylpyrrolidone (PVP, 1 mmol) was added under vigorous stirring. After continuous stirring for 3 h, the as-prepared mixture was reduced by adding an aqueous solution of sodium borohydride ($NaBH_4$, 0.8 mmol, 5 ml) with vigorous stirring for 2 h. The resulting mixture was dialyzed in water using a dialysis tube for 4 h to yield SPtNP catalysts. The formation of PtNPs is proven by powder XRD (Fig. S1†). The diffraction peaks at 39.9°, 46.7°, and 68.4° can be assigned to the (111), (200), and (220) planes of the face-centered cubic Pt particles, respectively. The XRD results revealed that the peaks of NaCl at 45.5°, 66.3° and 75.4° disappeared after dialysis by comparing Fig. S1 and S2.†

The molar ratio of Pt to PVP was varied in the range of 1/1 to 1/100 to study the roles of the stabilizers in SPtNP catalysts. High-resolution transmission electron microscopy (HRTEM) characterization shows that the sizes of the PtNPs were dependent on the molar ratio of Pt to PVP (Fig. 1, S5, and S6† and Table 1). Particle size distributions are accompanied by a peak function fitted to the histograms with the R^2 associated with the fitting being approximately 0.99. When the molar ratio of Pt/PVP is 1 : 1, the PtNPs are well-dispersed with a mean size of 3.5 nm and a narrow distribution, which indicated that PVP plays a role in stabilizing PtNPs. By increasing the molar ratio of Pt to PVP from 1/1 to 1/100, the diameters of Pt NPs decrease from 3.5 nm to 2.8 nm. The results indicate that with the increasing amount of PVP, more stabilizers will coat the surfaces of PtNPs, improving the stability of PtNPs, which prevents PtNP aggregation and thus reduces the sizes of PtNPs. Fig. S5c† presents the results of the HRTEM images, clearly showing two kinds of crystal planes. The interplanar spacings are measured to be 0.229 and 0.198 nm, which are characteristic of (111) and (200) lattice planes of face-centered cubic Pt, respectively.

The added amounts of stabilizer not only affect the sizes of PtNPs but also further have a significant effect on the activity of

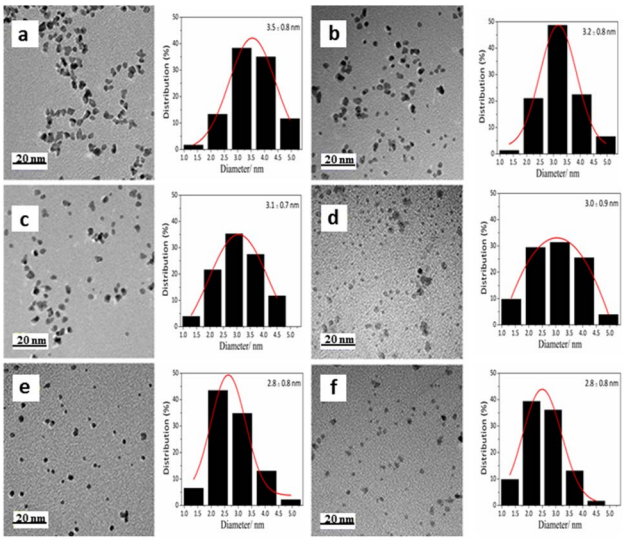

Fig. 1 TEM images and size distributions of the freshly prepared SPtNP catalysts with different molar ratios of Pt to PVP: (a) 1 : 1, (b) 1 : 5, (c) 1 : 10, (d) 1 : 20, (e) 1 : 50, and (f) 1 : 100.

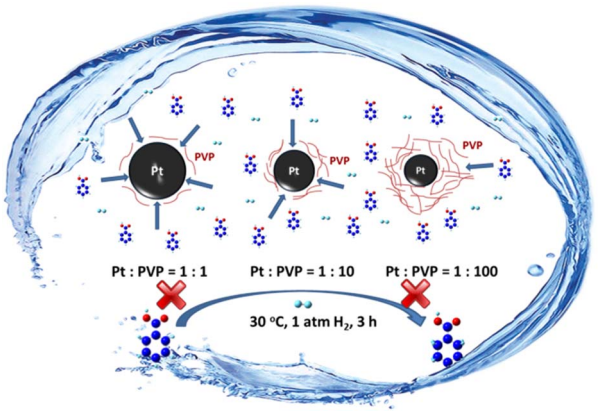

Scheme 1 One-step selective conversion of BA to CCA under mild conditions catalyzed by the SPtNP catalyst prepared with a suitable stabilizer and reductant.

Table 1 Results of hydrogenation of BA by the SPtNP catalysts prepared with different stabilizers and reductants[a]

Entry	Pt : PVP (mol%)	Reductants	Size (nm)	C^b (%)	S^c (%)
1	1 : 1	$NaBH_4$	3.5	72.1	100
2	1 : 5	$NaBH_4$	3.2	84.6	100
3	1 : 10	$NaBH_4$	3.1	100	100
4	1 : 20	$NaBH_4$	3.0	62.1	100
5	1 : 50	$NaBH_4$	2.8	56.9	100
6	1 : 100	$NaBH_4$	2.8	46.2	100
7	1 : 10	Ethanol	3.3	78.4	100
8	1 : 10	Formaldehyde	2.8	50.6	100
9	1 : 10	Hydrazine hydrate	80.0	0.0	0
10	Pt/C	—	3.1	38.4	100
11	Pt/C[d]	—	3.1	32.6	100

[a] Reaction conditions: 5 mol% metal relative to BA, 30 °C, 1 atm H_2, 3 h. [b] BA conversions. [c] Selectivities of CCA. [d] Adding PVP (Pt : PVP = 1 : 10).

SPtNP catalysts, as shown in Table 1. 100% BA conversion under mild conditions (30 °C and 1 atm H_2 for 3 h, which is among the mildest condition for the selective hydrogenation of BA to CCA thus far) is only obtained on the SPtNP catalysts with the Pt : PVP molar ratio of 1 : 10 (Table 1, entry 3). The decrease in the BA conversion with decreasing the amount of PVP (*i.e.*, Pt : PVP>1 : 10) may be due to the growth in the diameter of the PtNPs. Such size effect was found prevalently with NP catalysts for many reactions,[9] which was generally ascribed to the existence of more coordinatively unsaturated sites on smaller particles and the changes in their electronic properties. By increasing the amount of stabilizer, the conversion of BA would also decrease. This is quite a confusing phenomenon to understand, as the diameters of PtNPs reduce with increasing the added amount of PVP. However, it is speculated that, with the excess amount of PVP (*i.e.* Pt : PVP<1 : 10), the drop of the conversion may be due to the covering of the active Pt sites with excess PVP molecules, which block the access of BA to active Pt sites, leading to reduced catalytic activity (Scheme 1). These results reveal that the stabilizer (PVP) not only protects the outer surfaces of prefabricated PtNPs, affecting their sizes, but has significant effects on the accessibility of active metal sites, which determines the activity of catalysts.

To unveil the role of reductants in SPtNP catalysts in the selective hydrogenation of BA, the activities of SPtNP catalysts prepared with different reductants were investigated. As shown in Table 1, the Pt NPs reduced by ethanol, formaldehyde, and hydrazine hydrate yielded much lower BA conversions (78.4% for ethanol, 50.6% for formaldehyde, and 0% for hydrazine hydrate) compared with $NaBH_4$. TEM characterization of these catalysts reduced by different reductants showed that they possessed similar metal particle sizes (2.8–3.3 nm) except that reduced by hydrazine hydrate (Fig. S3†). The diameter of PtNPs reduced by hydrazine hydrate (~80 nm) is much larger than that of others, which resulted in them being unavailable for catalysis. When formaldehyde is used as a reductant, the PtNPs possess a smaller diameter (~2.8 nm) than those using $NaBH_4$ but have lower catalytic activity. A structural characterization using XPS implicated the change of surface electron structures of PtNPs as the possible origin of this decrease in catalytic activity, as is discussed below.

From XPS characterization of PtNPs (Fig. 2), the Pt 4f spectrum of the PtNPs reduced by $NaBH_4$ is resolved into two peaks with a $4f_{7/2}$ binding energy of 74.7 eV and a $4f_{5/2}$ binding energy of 71.4 eV (Fig. 2a), verifying the presence of metallic Pt (Pt(0)) in the catalysts. The absence of Pt(II) and Pt(IV) related diffraction peaks demonstrates the complete reduction of Pt(IV) precursors to exclusively metallic Pt(0) species. On the other hand, the Pt 4f spectrum of the PtNPs reduced by ethanol (Fig. 2b) shows two new signals of the oxidation state of Pt (Pt(II)) at 75.0 (Pt $4f_{7/2}$) and 71.9 eV (Pt $4f_{5/2}$), indicating that the Pt precursor cannot be reduced completely. The ratio of Pt(0) to Pt(II) is 2.27 : 1. In particular, the intensities of Pt(II) in the Pt 4f spectrum (Fig. 2c) for the Pt NPs reduced by formaldehyde are much stronger (the ratio of Pt(0) to Pt(II) is 1.36 : 1) than those using $NaBH_4$ and ethanol as reductants, showing that Pt(II) content is much higher in this catalyst, resulting in a decrease in catalytic activity.

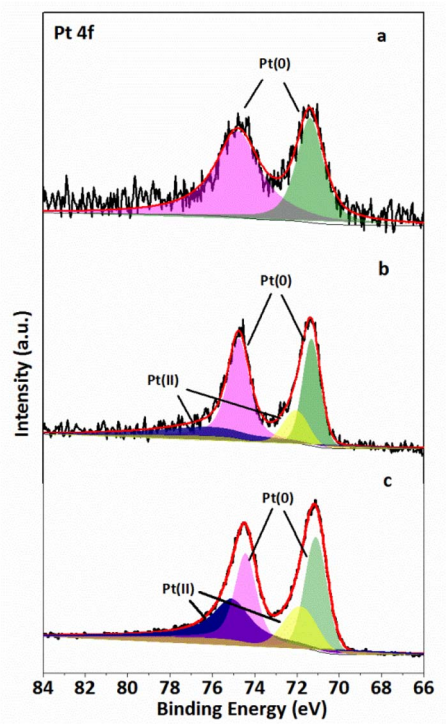

Fig. 2 XPS spectra of the SPtNP catalysts reduced by (a) $NaBH_4$, (b) ethanol, and (c) formaldehyde at a Pt : PVP molar ratio of 1 : 10.

By studying the roles of the stabilizer and reductant, we found that size effects are not the only factor that determines the activity of catalysts, and the electronic state and accessibility of the active metal sites are also very important factors. The SPtNP catalyst prepared with a suitable stabilizer and reductant presents significantly high catalytic activity in mild conditions (Table 1, entry 3). For comparison, 5 wt% Pt/C was examined in the hydrogenation of BA (Table 1, entry 10), which showed a lower BA conversion (38.4%). The diameter of Pt (3.1 nm) in Pt/C is similar to that in SPtNP catalysts (Fig. S3†), which indicates that the size effect of PtNPs is not the reason for the decrease in activity. However, the poor dispersion in solution and high liquid–solid mass transfer resistance lead to a decline in the activity of the catalyst. The addition of PVP with 5 wt% Pt/C catalyst (Pt : PVP = 1 : 10) led to little decrease in the BA conversion from 38.4 to 32.% (Table 1, entry 11), most likely due to the covering of active Pt sites by PVP. Furthermore, compared with the catalysts in the previous literature (Table S3†), the SPtNP catalyst prepared with a suitable stabilizer and reductant shows excellent catalytic activity for the selective hydrogenation of BA to CCA under the mildest reaction conditions (30 °C and 1 atm H_2) thus far.

Diethyl ether features remarkable immiscibility with water. The SPtNP catalyst can be easily separated by extracting the product with diethyl ether for recyclability tests. After extraction, the remaining SPtNP catalyst in water is seamlessly recycled for further reactions. The BA conversion and selectivity

remain essentially constant, being above 99%, after recycling the SPtNP catalyst over five times (Fig. S4†), demonstrating the excellent stability of the SPtNP catalyst. TEM characterization results (Fig. S5†) show no obvious growth or aggregation for the used SPtNP catalyst. The SPtNP catalyst shows excellent activity, durability, and stability in the water-phase catalytic reaction.

To illustrate the catalytic properties of the SPtNP catalyst in detail, the method was extended to ring hydrogenation of as many as eight benzoic acid derivatives, and the results are presented in Table 2. The SPtNP catalyst shows excellent activity for the hydrogenations of phenylacetic acid and other benzoic acid derivatives, including benzamide, methyl benzoate, and so on. Furthermore, 100% conversion of phenylacetic acid is obtained over the SPtNP catalyst (Table 2, entry 1). Then, the hydrogenations of p-substituted benzoic acids (–CH_3, –Br, –Cl, –OH, and –OCH_3) are investigated. The conversion of the hydrogenation of p-methyl benzoic acid is 23.8% at 30 °C and 1 atm H_2 for 3 h (Table 2, entry 2), which is much lower than that of benzoic acid. The conversion increases to 100% by increasing the reaction temperature to 60 °C and prolonging the reaction time to 6 h. The hydrogenations of *p*-bromobenzoic acid and *p*-chlorobenzoic acid exhibit conversion of 86.0% and 64.3% at 30 °C and 1 atm H_2 for 3 h, respectively (Table 2, entries 3 and 4). The hydrogenation of *p*-bromobenzoic acid is prolonged to 4 h with a conversion of 100%, and that of *p*-chlorobenzoic acid is prolonged to 6 h with a conversion of 100%. Meanwhile, the hydrogenations of *p*-halobenzoic acids don't give the anticipated *p*-halohexanecarboxylic acids as the final products, but rather, hexanecarboxylic acid is the only product. It is known that the halo moiety of the aromatics is usually easily reduced under hydrogen pressure, and this applies to the above-mentioned case.[10] The results prove that the Br group is a better leaving group than the Cl group in this system. Hydrogenations of *p*-hydroxybenzoic acid and *p*-anisic acid exhibit conversion of 45.0% and 7.8% with two products (hexahydrobenzoic acid and *p*-substituted hexahydrobenzoic acid), respectively, at 30 °C and 1 atm H_2 for 3 h (Table 2, entries 5 and 6). The results show that the oxygen-containing p-substituted groups (hydroxyl groups and methoxyl group) can react with H_2 to leave. It is also favorable to increase the conversion (100%) through longer reaction time and higher temperature. Hydrogenations of *p*-hydroxybenzoic acid and *p*-anisic acid are separated into two steps: benzene hydrogenation and then p-substituted group reaction, in which higher temperature and longer time would result in faster reaction. The SPtNP catalyst shows excellent activity on hydroxylic acid and benzene ester compounds, and amide compounds. 44.0% conversion of benzamide and 77.2% conversion of methyl benzoate are obtained over the SPtNP catalyst (Table 2, entries 7 and 8). Extending the reaction time can improve the conversion to 100%. In general, the SPtNP catalyst has excellent catalytic activity for benzoic acid derivatives. The introduction of electron-donating groups to benzene rings substantially enhances the aromatic system's electron density through combined inductive and conjugative effects. This elevated electron density amplifies repulsive interactions between the π-cloud and approaching hydrogen atoms during hydrogenation, thereby significantly increasing the activation energy barrier and rendering the hydrogenation process more thermodynamically challenging (Table 2, entries 2, 7, and 8). Notably, the presence of labile functional groups on the aromatic ring facilitates deep hydrogenation through concurrent bond cleavage events. Comparative analysis reveals distinct reactivities among functional groups: Halogens demonstrate exceptional leaving-group propensity under hydrogenation conditions, whereas carbon–oxygen bonds exhibit remarkable persistence due to their higher bond dissociation energy. The inherent stability of C–O bonds creates additional kinetic barriers through two complementary mechanisms, both by resisting activation itself and by maintaining electronic perturbations that disfavor the hydrogenation pathway (Table 2, entries 3–6).

Table 2 Hydrogenation of benzoic acid derivatives[a]

	Substrate	Product	T (°C)	t (h)	C^b (%)	S^c (%)
1	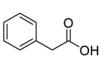	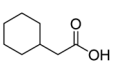	30	3	100	100
2	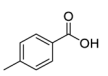	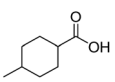	30(60)	3(6)	23.8(100)	100
3	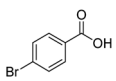	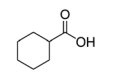	30	3(4)	86.0(100)	100
4	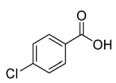	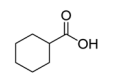	30	3(6)	64.3(100)	100
5	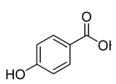	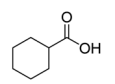	30(60)	3(10)	45.0(100)	100
6	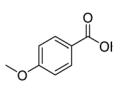	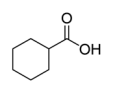	30(60)	3(10)	7.8(100)	100
7	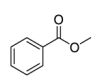	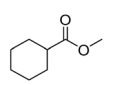	30	3(5)	77.2(100)	100
8	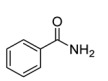	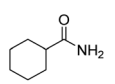	30	3(8)	44.0(100)	100

[a] Reaction conditions: 5 mol% Pt relative to substrates, 1 atm H_2, 30 °C, 3 h, Pt : PVP = 1 : 10. [b] Conversions. [c] Selectivities.

Conclusions

In summary, the amount of stabilizers and the type of reductants can dramatically influence not only the size but also the electronic state and accessibility of active metal sites, which have great effects on catalytic activity. The SPtNP catalyst prepared with a suitable stabilizer and reductant presented significantly high catalytic activity for the chemo-selective hydrogenation of BA to CCA at atmospheric pressure and ambient temperature in water, whereas at the same reaction conditions, a low yield of CCA was obtained over Pt/C. The

hydrogenations of benzoic acid derivatives were also investigated to illustrate the general applicability of the SPtNP catalyst, and the substituent is believed to be of great influence on the reaction rate.

Data availability

The data supporting this article have been included as part of the ESI.†

Conflicts of interest

There are no conflicts to declare.

Acknowledgements

The financial support of the China Postdoctoral Science Foundation (No. 2021M702435) is gratefully acknowledged. We thank the comprehensive training platform of the specialized laboratory, College of Chemistry, Sichuan University, for the instrumental measurement.

Notes and references

1 (*a*) N. Yan, C. X. Xiao and Y. Kou, *Coord. Chem. Rev.*, 2010, **254**, 1179–1218; (*b*) Y. B. Huang, Q. Wang, J. Liang, X. Wang and R. Cao, *J. Am. Chem. Soc.*, 2016, **138**, 10104–10107; (*c*) X. C. Yang, J. K. Sun, M. Kitta, H. Pang and Q. Xu, *Nat. Catal.*, 2018, **1**, 214–220; (*d*) G. Chacón and J. Dupont, *ChemCatChem*, 2019, **11**, 333–341.

2 (*a*) C. X. Xiao, Z. P. Cai, T. Wang, Y. Kou and N. Yan, *Angew. Chem., Int. Ed.*, 2008, **47**, 746–749; (*b*) J. G. Zhang, H. Asakura, J. V. Rijn, J. Yang, P. Duchesne, B. Zhang, X. Chen, P. Zhang, M. Saeys and N. Yan, *Green Chem.*, 2014, **16**, 2432–2437; (*c*) J. F. Zhu, G. H. Tao, H. Y. Liu, L. He, Q. H. Sun and H. C. Liu, *Green Chem.*, 2014, **16**, 2664–2669; (*d*) H. Y. Liu, Q. Q. Mei, Y. Y. Wang, H. Z. Liu and B. X. Han, *Sci. China Chem.*, 2016, **59**, 1342–1347; (*e*) H. Mao, Y. Liao, J. Ma, S. L. Zhao and F. W. Huo, *Nanoscale*, 2016, **8**, 1049–1054.

3 Y. Z. Wang, S. De and N. Yan, *Chem. Commun.*, 2016, **52**, 6210–6224.

4 J. Ding, Y. F. Bu, M. Ou, Y. Yu, Q. Zhong and M. H. Fan, *Appl. Catal., B*, 2017, **202**, 314–325.

5 (*a*) S. Y. Yao, Y. Yuan, C. X. Xiao, W. Z. Li, Y. Kou, P. J. Dyson, N. Yan, H. Asakura, K. Teramura and T. Tanaka, *J. Phys. Chem. C*, 2012, **116**, 15076–15086; (*b*) S. S. Acharyya, S. Ghosh, R. Tiwari, B. Sarkar, R. K. Singha, C. Pendem, T. Sasaki and R. Bal, *Green Chem.*, 2014, **16**, 2500–2508; (*c*) U. T. Khatoon, A. Velidandi and G. V. S. N. Rao, *Mater. Chem. Phys.*, 2023, **294**, 126997; (*d*) C. B. Norris, P. R. Joseph, M. R. Mackiewicz and S. M. Reed, *Chem. Mater.*, 2010, **22**, 3637–3645; (*e*) A. Stolaś, I. Darmadi, F. A. A. Nugroho, K. Moth-Poulsen and C. Langhammer, *ACS Appl. Nano Mater.*, 2020, **3**, 2647–2653; (*f*) S. Ghosh, S. K. Sharma, S. Rana, T. S. Khan, T. Sasaki, S. S. Acharyya and R. Bal, *ACS Appl. Nano Mater.*, 2023, **6**, 17668–17680.

6 (*a*) H. Shinkai, K. Toi, I. Kumashiro, Y. Seto, M. Fukuma, K. Dan and S. Toyoshima, *J. Med. Chem.*, 1988, **31**, 2092–2097; (*b*) H. Shinkai, M. Nishikawa, Y. Sato, K. Toi, I. Kumashiro, Y. Seto, M. Fukuma, K. Dan and S. Toyoshima, *J. Med. Chem.*, 1989, **32**, 1436–1441; (*c*) B. S. Moore, H. Cho, R. Casati, E. Kennedy, K. A. Reynolds, U. Mocek, J. M. Beale and H. G. Floss, *J. Am. Chem. Soc.*, 1993, **115**, 5254–5266.

7 J. Ritz, H. Fuchs, H. Kieczka and W. C. Morgan, *Ullmanns Encyclopedia of Industrial Chemistry*, Wiley-VCH, 2001.

8 (*a*) G. Y. Bai, X. Wen, Z. Zhao, F. Li, H. X. Dong and M. Qiu, *Ind. Eng. Chem. Res.*, 2013, **52**, 2266–2272; (*b*) G. Bai, Z. Zhao, H. Dong, L. Niu, Y. Wang and Q. Chen, *ChemCatChem*, 2014, **6**, 655–662; (*c*) X. Wen, Y. Y. Cao, X. L. Qiao, L. B. Niu, L. Huo and G. Y. Bai, *Catal. Sci. Technol.*, 2015, **5**, 3281–3287; (*d*) H. L. Zhang, X. J. Gao, Y. Y. Ma, X. Han, L. B. Niu and G. Y. Bai, *Catal. Sci. Technol.*, 2017, **7**, 5993–5999; (*e*) Z. L. Jiang, G. J. Lan, X. Y. Liu, H. D. Tang and Y. Li, *Catal. Sci. Technol.*, 2016, **6**, 7259–7266; (*f*) X. H. Lua, Y. Shen, J. He, R. Jing, P. P. Tao, A. Hua, R. F. Nie, D. Zhou and Q. H. Xia, *Mol. Catal.*, 2018, **444**, 53–61; (*g*) H. Z. Jiang, X. L. Yu, R. F. Nie, X. H. Lu, D. Zhou and Q. H. Xia, *Appl. Catal., A*, 2016, **520**, 73–81; (*h*) M. Tang, S. Mao, M. Li, Z. Wei, F. Xu, H. Li and Y. Wang, *ACS Catal.*, 2015, **5**, 3100–3107; (*i*) C. Chaudhari, H. Imatome, Y. Nishida, K. Sato and K. Nagaoka, *Catal. Commun.*, 2019, **126**, 55–60; (*j*) H. L. Zhang, J. Dong, X. L. Qiao, J. R. Qin, H. F. Sun, A. Q. Wang, L. B. Niu and G. Y. Bai, *J. Catal.*, 2019, **372**, 258–265; (*k*) W. J. Lian, B. Chen, B. Y. Xu, S. Zhang, Z. Wan, D. Zhao, N. Zhang and C. Chen, *Ind. Eng. Chem. Res.*, 2019, **58**, 2846–2856; (*l*) R. F. Nie, H. Z. Jiang, X. H. Lu, D. Zhou and Q. H. Xia, *Catal. Sci. Technol.*, 2016, **6**, 1913–1920; (*m*) X. Yang, L. Du, S. Liao, Y. Li and H. Song, *Catal. Commun.*, 2012, **17**, 29–33; (*n*) H. W. Lin, C. H. Yen and C. S. Tan, *Green Chem.*, 2012, **14**, 682–687; (*o*) H. J. Wang and F. Y. Zhao, *Int. J. Mol. Sci.*, 2007, **8**, 628–634; (*p*) Y. L. Cao, M. H. Tang, M. M. Li, J. Deng, F. Xu, L. Xie and Y. Wang, *ACS Sustain. Chem. Eng.*, 2017, **5**, 9894–9902; (*q*) Z. Guo, L. Hu, H. H. Yu, X. Cao and H. Gu, *RSC Adv.*, 2012, **2**, 3477–3480; (*r*) H. F. Zhang, G. Q. Li, R. F. Nie, X. H. Lu and Q. H. Xia, *J. Mater. Sci.*, 2019, **54**, 7529–7540; (*s*) J. J. Shi, M. S. Zhao, Y. Y. Wang, J. Fu, X. Y. Lu and Z. Y. Hou, *J. Mater. Chem. A*, 2016, **4**, 5842–5848; (*t*) X. Xu, M. H. Tang, M. M. Li, H. R. Li and Y. Wang, *ACS Catal.*, 2014, **4**, 3132–3135; (*u*) M. H. Tang, S. J. Mao, X. F. Li, C. H. Chen, M. M. Li and Y. Wang, *Green Chem.*, 2017, **19**, 1766–1774; (*v*) D. Chen, W. Yang, L. Jiao, L. Li, S. H. Yu and H. L. Jiang, *Adv. Mater.*, 2020, 2000041.

9 (*a*) S. Dang, Q. L. Zhu and Q. Xu, *Nat. Rev. Mater.*, 2018, **3**, 17075; (*b*) X. C. Kang, H. Z. Liu, M. Q. Hou, X. F. Sun, H. L. Han, T. Jiang, Z. F. Zhang and B. X. Han, *Angew. Chem., Int. Ed.*, 2016, **55**, 1080–1084.

10 B. J. Yao, Q. J. Fu, A. X. Li, X. M. Zhang, Y. A. Li and Y. B. Dong, *Green Chem.*, 2019, **21**, 1625–1634.